Ocean Sci. Discuss., https://doi.org/10.5194/os-2017-86
Manuscript under review for journal Ocean Sci.
Discussion started: 21 June 2018

Ocean Science Discussions

Monitoring of seasonally variability and movement of suspended sediment concentration along Thiruvananthapuram coast using OLI sensor

Bismay Ranjan Tripathy[1], Kaliraj Seenipandi[1], Haroon Sajjad[2], Pawan Kumar Joshi[3], Bhagwan Singh Chaudhary[4] and Pavan Kumar[2,*]

[1]National Centre for Earth Science Studies, Thiruvananthapuram - 695011, India
[2]Department of Geography Jamia Millia Islamia, New Delhi, India
[3]School of Environmental Science, Jawaharlal Nehru University, New Delhi, India
[4] Department of Geophysics, Kurukshetra University, Kurukshetra, Haryana, India

Correspondence to: Pavan Kumar (pavan.jamia@gmail.com)

Abstract. In the recent decades hydrologists, geologists, and stream ecologists have shown substantial interest in analyzing suspended sediments in water. Extracting information like suspended sediment concentration (SSC) in coastal waters is very important for assessment and monitoring of coastal settings and their effects on their ecology. This article demonstrates importance of Landsat 8 Operational Land Imager (OLI) for monitoring seasonal variation in SSC and movement (pre and post monsoon) along Thiruvananthapuram coast in India. The data was converted into marine reflectance after correcting due atmospheric errors. SSC was extracted using spectral analysis data analysis. Movement of SSC was monitored using wave direction and significant wave height data. The results revealed that the SSC decreased rapidly with the increase in distance from the beach and depth of the seabed. Wave with higher frequency in deeper water caused sparely circulation of sediments and their concentration at the lower depth in high bathymetry. Thus, the suspended sediments were indirectly proportional to bathymetry and distance from the shoreline and directly proportion to wave direction and littoral current at off-shore. High concentration of sediments was found to be accumulated at shallow depth (< 10m), which was estimated to be 92 mg/l and decreased up to 30mg/l at a depth of 30 m. The movement of sediments was observed north-south during the pre-monsoon and reversed during post-monsoon due to reversal in wind direction. Satellite remote sensing techniques and data processing can be efficiently used for SSC monitoring and their movement in ocean. Such estimates over temporal and spatial scales can be used for coastal zone management and conservation.

1 Introduction

Suspended loads are generally the portion of sediments, which contain fine sand, silt and clay etc and are carried to the ocean by the action of the fluid. These particles settle in such a way that they certainly do not touché the bed, which is maintained

Ocean Sci. Discuss., https://doi.org/10.5194/os-2017-86
Manuscript under review for journal Ocean Sci.
Discussion started: 21 June 2018

by means of turbulence of flowing water. Therefore, it is necessary to measure and monitor the suspended sediments in the ocean transported by various agents for flood hazard management, water resource planning, climate and ecology studies (Whitelock, *et al*., 1981; Sinha *et al*., 2004). A large number of noteworthy researches have been conducted on the spatiotemporal deviation in suspended sediments concentration (SSC) in a system all over the world (Kaliraj and Chandrasekar, 2012). However, monitoring and measurement of such suspended sediments is extremely difficult due to dynamic unit distance and factors acting on it. . Consequently since the last few decades, attention has been paid to the potential of satellite data to measure and monitor the movement of SSC in ocean (Nechad, *et al.* 2010; Ontowirjo, *et al*., 2013; Rawat *et al*., 2011; Curran *et al*., 1988). Remote sensing offers larger aerial view for analyzing water quality and provides a more efficient cost effective method for assessing SSC from the ocean. Geospatial technology has been widely used by many hydrologists, as it has the ability to answer complex, spatial and temporal questions. (Marcus and Fonstad, 2010; Panwar *et al*., 2017).

Presently satellite technology is opted over marine surveys to assess the distribution and movement of suspended sediments because the cost of application is lower than that of site marine survey as it replaces the requirement for a large number of monitoring positions with a single satellite (Byers, 1992). It performs as an influential tool for mapping suspended sediments in the ocean, which has been discharged by a various sources like; river, stream, industries and urban residues. Images taken by optical devices boarded on the satellites and field observation data help in regular monitoring of suspended sediment transportation (Gerald, 1980; Kaliraj and Chandrasekar, 2012). However, it is hindered by two vital difficulties. First, remotely sensed data can detect the suspended sediments in the upper few meters of the water layers. Thus it is necessity to convert it into a depth-integrated load before evaluation for numerical models and field measurements. Second, numerous approaches are dependent on the observed relationship between water-leaving reflectance and SSC analyzed through remote sensing tools. Experimental corrections provide site-specific calculations of water quality parameters with practical accuracy by using field derived reflectance data. Spectral examination of satellite imagery is based on the calculation of reflected electromagnetic solar radiation, which is used to evaluate turbidity and SSC. Depending on reflection and absorption of different wavelengths, unique signature and curves are produced (Islam, *et al*., 2001; Kaliraj, *et al*., 2013a; Kaliraj, *et al*., 2013b).

Remotely sensed data can only provide information in one-two dimensional forms because, it cannot give evidence on the vertical circulation of sediments in water as we get the reflection data from only two-meter surface water (Tassan, 1998). Two/three-dimensional information using remote sensing data is of less value as the data is not vertically averaged. Oceanic survey, on the other hand, can be modeled for three dimensions as it is the average data of vertically through the water column to horizontally across the surface of the water. Thus, a comprehensive series of sample acquisition throughout the water column is essential for assessing the vertical sediment distribution (Katlane, *et al*., Katlane, *et al*., 2013; Warrick *et al*., 2014). Wavelength between 0.5 and 0.8m is used for remote sensing for detecting suspended sediments, which includes the

Ocean Sci. Discuss., https://doi.org/10.5194/os-2017-86
Manuscript under review for journal Ocean Sci.
Discussion started: 21 June 2018

visible, green, red and near infra-red light. Colour and turbidity in the water, affect the energy level (visible, very near ultraviolet and infra-red wavelengths) which is sensed by a camera or scanner. Energy flux decreases with increase in colour (due to absorption of solar energy) and the flux increases with an increase in turbidity (due to reflection of solar energy). As solar energy is reflected but that sensed data cannot be used directly as it contains atmospheric errors, which need to be corrected before its further use (Wang and Lu 2010; Qu, 2014). The study makes an attempt to monitor the suspended sediments, using Landsat 8 (OLI) at Thiruvananthapuram district coast; we first corrected atmospheric errors in the data and then converted it into marine reflectance. The specific objectives of the study were to monitor seasonal variation in suspended sediment concentration and to assess movement of suspended sediments during pre and post-monsoon. The other objective was to map the coastal landforms and their changes.

2 Study area

The coastal zone of the Thiruvananthapuram District of Kerala in India covers a stretch of about 72km extending seaward for 10 km from the coast bound. The geographical extent of the area is between 8°17' N and 8°54' N latitudes and 76°41' E and 77°17' E longitudes (Fig. 1). The coastal stretch is highly dynamic due to the hydrodynamic forces such as waves, currents and tides, etc. It has also undergone changes in near shore bathymetry and landforms. The landforms along the coast experienced morphological instability due to both natural and anthropogenic factors. Commercial activities, tourist's sites, dense population and thick settlement are characteristic features of major locations of the coastal stretch. Along the coast, human settlements and properties are threatened due to severe coastal erosion. The study area experiences a sub-tropical climate with average annual rainfall varying from 826 mm to 1456 mm and the annual mean temperature ranging from 23.78 ^{0}C to 33.95^0 C.

<Insert Fig. 1 Location map of study area>

3 Material and methodology

3.1 Data used

We used OLI data for determining pre-monsoon (March 2017) and post-monsoon (September 2017) suspended sediments. Operation Land Imager gives the multispectral data for visible as well as infrared range. It covers the entire earth in 16 days. The OLI uses the push broom sensor with 115-mile cross-track field of view.

Digital Bathymetry Model (DBM) was utilized for extracting the bathymetry. Shuttle radar topography mission is a research effort that obtained digital elevation model for generating high-resolution digital topography database for the earth. For extracting the bathymetry, we have used a global relief model which composite model of Digital Bathymetry Model (DBM). SRTM30_PLUS (http://topex.ucsd.edu/WWW_html/srtm30_plus.html) consists of both topography and bathymetry model

Ocean Sci. Discuss., https://doi.org/10.5194/os-2017-86
Manuscript under review for journal Ocean Sci.
Discussion started: 21 June 2018

that provides 30arc seconds (900m) resolution data for land as well as for Ocean, which is derived from depth sounding (SONAR) and satellite altimetry. Finally, the wind direction is derived from the portal ERA (European Reanalysis) Interim, provided by ECMWF (European Centre for Medium-Range Weather Forecasts), which is an independent intergovernmental organisation, based on a four-dimensional IFS (Cy31r2) system.

3.2 Conversion of DN to TOA reflectance

Atmospheric correction was done to determine the water-leaving reflectance (ratio of upwelling radiance just above the water surface and the solar down welling irradiance) by eliminating the contribution of surface glint and atmospheric scattering from the estimated total reflectance. The total atmospheric reflectance was estimated as the sum of the molecular reflectance (Rayleigh's reflectance), specular reflection of the sun and the reflectance of aerosol, foam and whitecaps. All these parameters were determined from the metadata and field measurement, using empirical relationship (Gordon and Wang, 1994). Solar radiation is totally absorbed by water in NIR band. Thus, water-leaving radiance can be eliminated to estimate aerosol directly. Hence, medium to relatively high suspended particulate matter (SPM) concentration can better be mapped by using near-infrared and red bands.

These raw data can be converted to ToA Reflectance from DN (eq.i), using rescaling factors and parameters found in the metadata file (MTL.txt) provided with the data.

$$\rho_t^{'} = (M_p)(Q_{cal}) + (A_r) \quad \text{(i)}$$

Where;
$\rho_t^{'}$= TOA planetary reflectance (without solar angle correction)
M_p= Band-specific multiplicative rescaling factor
A_r =Band-specific additive rescaling factor
Q_{cal}= Quantized and calibrated standard product pixel values (DN)

Next, we have corrected the $\rho_t^{'}$ using eq. ii for the solar angle;

$$\rho_t = \frac{\rho_t^{'}}{\cos(\theta_{SZ})} = \frac{\rho_t^{'}}{\sin(\theta_{SE})} \quad \text{(ii)}$$

Where;
ρ_t = TOA planetary reflectance
θ_{SE}= Local sun elevation angle
θ_{SZ}= Local solar zenith angle
θ_{SZ}= 90° - θ_{SE}.

Ocean Sci. Discuss., https://doi.org/10.5194/os-2017-86
Manuscript under review for journal Ocean Sci.
Discussion started: 21 June 2018

3.3 Molecular/ Rayleigh's reflectance correction

Most Reflectance from air molecules and aerosols must be accurately modeled and removed from the observed signal. At-sensor total reflectance (eq.iii) can be expressed as the following formula.

$$\rho_{TOA} = \frac{L_1B\_Radiance}{Extra\ Terrestrial\ Sun\ Radiation} \quad \text{(iii)}$$

After the Rayleigh correction, ground surface + aerosol albedo r_{as} can be determined as :

$$\rho_{0.5} = [\,\rho_{TOA} - \rho_R/T_R]/\,[1 + S_R\,(\rho_{TOA} - \rho_R/T_R)] \quad \text{(iv)}$$

Where;

ρ_r= Rayleigh reflectance

Extra Terrestrial Sun Radiation $= (\pi)(E_S)(\cos(\theta_S))\,(d_{sol})\exp\,[(-m)(\tau_{net})]$

$$m = \frac{1}{\cos\,(\theta_s)} + \frac{1}{\cos\,(\theta_v)}$$

θ_s and θ_v are the angle of solar zenith and sensor zenith respectively

d_{sol} is the eccentricity correction factor of the earth' s orbit

T_R = Rayleigh atmospheric transmittance

$$T_{total} = (\mathrm{T}_{yu})(\,\mathrm{T}_{yd})\,\exp\,[(-m)(\tau_{O_2})]\,\exp\,[(-m)(\tau_{water\ vapour})]$$

T_{yu} =Rayleigh transmittance for sensor

$$\mathrm{T}_{yu} = \frac{2/3 + \cos(\theta_v) + (2/3 - \cos(\theta_v))\,\exp\,[-(\tau_{Raylight})/(\cos\,(\theta_v)]}{4/3 + \tau_{Raylight}}$$

T_{yd} = Rayleigh transmittance for sun

$$\mathrm{T}_{yd} = \frac{2/3 + \cos(\theta_s) + (2/3 - \cos(\theta_s))\,\exp\,[-(\tau_{Raylight})/(\cos\,(\theta_s)]}{4/3 + \tau_{Raylight}}$$

Where;

$\tau_{Raylight}$ = Rayleigh optical depth

τ_{O_2} = Oxygen optical depth

τ = Optical depth

S_R= Rayleigh spherical albedo

Ocean Sci. Discuss., https://doi.org/10.5194/os-2017-86
Manuscript under review for journal Ocean Sci.
Discussion started: 21 June 2018

$$Ray\ Polynomi = -0.58 + \tau_{Raylight} - 0.25(\tau_{Raylight})^2 + 0.055(\tau_{Raylight})^3 - 0.0098(\tau_{Raylight})^4 + 0.0011(\tau_{Raylight})^5$$

Rayleigh reflectance (ρ_r) is calculated below;

$$\rho_r = (\mu_s, \mu_v, \emptyset_v - \emptyset_s) = \rho_{R1}(\mu_s, \mu_v, \emptyset_v - \emptyset_s) + (1 - \exp[-(\tau)/(\mu_v)] * (1 - \exp[-(\tau)/(\mu_v)]\Delta(\tau) \quad (v)$$

Where;
μ_s=cos of sun zenith
μ_v= cos of sensor zenith
$\emptyset_v$= sun azimuth
$\emptyset_s$= sensor azimuth
ρ_{R1}= the single-scattering contribution
τ = Atmospheric optical depth

Sensor spectral response based pre-computed radaitive transfer simulations, solar and sensor viewing geometry and ancillary information were used to estimate most of the components of the above equations. Rayleigh correction was executed by subtracting the Rayleigh reflectance value from the top of atmosphere reflectance as:

$$\rho_c = \rho_R - \rho_{TOA} \quad (vi)$$

3.4 Marine Reflectance Calculation

Aerosol reflectance (ε) was calculated from the ratio of reflectance in the couple of bands, over water pixels where the marine influence in those bands was expected to be zero. “ε"; the proportion of multiple-scattering aerosol reflectance was constant over the part. The value of ε was considered as 1 for getting standard processing in VR and NIR bands (Vanhellemont *et al*., 2014). The aerosol reflectance was projected by considering a linear relationship between marine reflectance of bands (VR and NIR) and constant aerosol type (ε) over the part. Aerosol can be extracted from the slope of the regression line (Neukermans, *et al*., 2009) or the median ratio of Rayleigh corrected reflectance in bands 4 and 5 (ρc^4, ρc^5) over clear water pixels. Alpha, “∝”, the ratio of oceanic reflectance was determined by using the average resemblance spectrum for the band central wavelengths:

Ocean Sci. Discuss., https://doi.org/10.5194/os-2017-86
Manuscript under review for journal Ocean Sci.
Discussion started: 21 June 2018

$$\propto = \frac{\rho_w{}^{(4)}}{\rho_w{}^{(5)}} = \frac{\bar{\rho}_{wn780}{}^{(655nm)}}{\bar{\rho}_{wn780}{}^{(865nm)}} = \frac{4.734}{0.544} = 8.702 \qquad \text{(vii)}$$

Gamma, "γ" is the fraction of diffused atmospheric transmittances in the two bands, which is calculated using the following equation (eq. viii).

$$\gamma = (t_0{}^{(4)})(t_v{}^{(4)})/(t_0{}^{(5)})(t_v{}^{(5)}) \qquad \text{(viii)}$$

Then, the oceanic reflectance is calculated using $\rho_w{}^{(3)}$and $\rho_w{}^{(4)}$ as noted eq. ix

$$\rho_w{}^{(3)} = \frac{\alpha}{t_0{}^{(4)} t_v{}^{(4)}}\left[\frac{\rho_c{}^{(3)} - \rho_c{}^{(4)}}{\alpha\gamma - \varepsilon}\right] \qquad \text{(ix)}$$

3.5 Spectralanalysis of the suspended sediments

The reflectance spectrum of an object is a graph of the radiation reflected to the incident wavelength and serves as a unique signature for the particular object. The water curve is characterized by a high absorption at near-infrared wavelength and beyond, whereas maximum reflectance at blue. The spectral curve for SSC is plotted for suspended particles in the ocean at a certain wavelength, after getting marine reflectance and correcting the aerosol from the data.

3.6 Extraction of suspended sediments

After getting the error free reflectance data, we have proceeded for mapping the movement of suspended sediments during pre-monsoon and post-monsoon seasons. In this paper, we have used a simple method to detect the area for OLI product based on the apparent reflectance of blue (0.45 - 0.51nm), red (0.64 - 0.67 nm) and near infrared (0.85 - 0.88 nm) µm wavelengths. Any increment of the red reflectance in the turbid water areas indicates the presence of sediment or shallow water. We determined suspended solid matter using the single band algorithm (eq.x) used by Nechad *et al*., 2010.

$$SPM = (A)(\rho_w/1) - (\rho_w)/c \qquad \text{(x)}$$

Where;
A = 327.84 g/m^3
C = 0.1708.

So in this way we have mapped the solid particles suspended near the shore (within 10 km) and get the idea about transportation of suspended particle along the coast during pre and post monsoon seasons.

Ocean Sci. Discuss., https://doi.org/10.5194/os-2017-86
Manuscript under review for journal Ocean Sci.
Discussion started: 21 June 2018

4 Results

The sources of suspended sediments are generally from the discharge of river, shore erosion and weathering of rocky shore. These sources control the creation of coastal headlands and provide source material to the physical, chemical and biological inputs in the offshore. The coastal region accumulated with suspended sediments changes the coastal morphology. The sediments near the shore are transported instead of being stable at a place due to various hydrodynamic action influences of the ocean such as mean significant wave height (Fig. 2). It is evident from the figure that the mean significant wave height is high for the southern part of the study area, which decreases towards the north. High wave energy can mingle more sediments in that region compared to less energy influential area, as it does not let the sediments transport to other places.

<Insert Fig. 2 Mean significant wave height along the coast>

4.1 Spectral signature of water and SSC having different magnitudes

The reflectance curve is plotted between the wavelength and the detected suspended sediments' reflectance from the large area of 900 sq. meters (30 meter resolution). The reflectance variation of the surface water indicates the presence of suspended sediments along the off-shore (Fig. 3). We can perceive that the regions having high suspended sediments have high reflectance in the NIR wavelength and the regions having comparatively less suspended sediments have high reflectance in the red wavelength. The area having no suspended sediments shows high reflectance in the blue wavelength and total absorption in the NIR wavelength. Hence reflectance curve helped to determine the concentration of suspended sediments in the water.

<Insert Fig. 3 Spectral reflectance of SSC in different wavelength of OLI image>

4.2 Monitoring of Suspended Sediments

The northern part of study area experienced heavy deposition during the post-monsoon as the suspended particles swashed by fewer energy waves along with the dominant wave direction in this session (Fig.4). Whereas, in the pre-monsoon, the circulation of the sediments found to be at lower part of the study area due to the dominate wave and current action along the shore (Fig. 5). Basically, a sediment particle will be suspended when the vertical velocity of the fluid motion becomes greater than the settling velocity of the particle. So, in the case of wave field, the vertical motion must result from the combined effects of turbulence and wave orbital motion. Here another phenomenon also acts on the sediments, i.e. gravity of the sediments suspended in the ocean, as the heavy sediments get deposited near shore, whereas the lighter sediments float. The wave direction in the post-monsoon and pre-monsoon is shown in Fig.4 and Fig. 5. It is found that SSC decreased rapidly with the increase in distance (0-10kilometers) from the shoreline as well as bathymetry level of 5-10 meters. Also, the effect of the wave shoaling in the deeper water is significantly less, which caused sparely distribution sediment

Ocean Sci. Discuss., https://doi.org/10.5194/os-2017-86
Manuscript under review for journal Ocean Sci.
Discussion started: 21 June 2018

concentration. The SSC, beyond 5000 meters from the shoreline and below 10-20 meters depth, are rarely observed as they cannot be measured at that depth, which is one of the limitations of the optical data. The movement of SSC indicates that the SSC have a positive correlation with wave direction and littoral current. We assigned weight to the layer based on the deposition along the shore. Most of the southern part of the study area was found to the high concentration of suspended matter during pre and post monsoon seasons. The middle part was found to have cyclic concentration as it experienced seasonal erosion of the shore and deposition sediments near the beach. The north most part of the study area was found have less concentration of the suspended sediments during pre and post monsoon seasons.

<Insert Figure 4 Suspended sediments in the pre monsoon >

<Insert Figure 5 Suspended sediments in the post-monsoon >

5 Discussion and Conclusion

The paper explored the concentration and movement of suspended particles along the Thiruvananthapuram coast. The findings revealed that p the sediment concentration decreased rapidly with the increase in distance to the beach and depth to the seabed. As the bathymetry increased, low amount of sediments available moved towards the shore to cause low concentrations in the surface water. Wave, frequent phenomena, at comparatively large distance in deeper water, caused sparely distribution of sediments. Thus, the sediments were concentrated at a lower depth in high bathymetry (≥10m) and distance more than 2 km from the shoreline. The dissimilarity of sediments revealed that the suspended sediments were indirectly proportional to bathymetry and distance from the shoreline and directly proportional to wave direction and littoral current at off-shore.

The study provides interesting visions for monitoring the suspended sediments at near shore after radiometric and geometric corrections. Another prospect of this study is the analysis of factors affecting the particles to be suspended in the near shore as well as offshore. OLI (30m) is having spectral range 0.45nm to 0.88 for visible as well as NIR, demonstrated the best details for spectral response analysis. This analysis revealed that the high reflection in near IR expressed the high concentration of SSC and, in contrast, the high reflection in the visible range showed lower concentration of suspended sediments. Suspended sediments moved north-south during post monsoon and reversed their direction during post monsoon season under the influence of monsoon winds. Mapping the spatial distribution of suspended materials using remotely sensed data would help in the management of coastal environment. Further study in this direction can aid the determination of the point and non- point source of water bodies, which discharge in the ocean. Hence, remote sensing data can potentially be utilized as a tool for monitoring the sediments in the ocean.

Acknowledgement:

The authors declare that there is no conflict of interests regarding the publication of this paper. BT, HS, BSC designed and proposed the research, BT, GSP processed data, PK, BT implemented techniques, PK, BT, PKJ analysed results, PK and BSC drafted and edited the article.

References

1. Byers, Alton C.: Soil loss and sediment transport during the storms and landslides of May 1988 in Ruhengeri prefecture, Rwanda, Natural Hazards, 5(3), 279-292, 1992.
2. Curran, P.J., and Novo, E.M.M.: The relationship between suspended sediment concentration and remotely sensed spectral radiance: a review, Journal of Coastal Research, 4(3), 351–368, 1988.
3. Gerald k. Moore: Satellite remote sensing of water turbidity / Sonde de télémesure par satellite de la turbidité de l'eau, Hydrological Sciences Bulletin, 25(4), 407-421, 1980.
4. Islam, M.R., Yamaguchi, Y., and Ogawa, K.: Suspended sediment in the Ganges and Brahmaputra River in Bangladesh: observation from TM and AVHRR data, Hydrological Processes, 15(3), 493–509, 2001.
5. Kaliraj, S., Chandrasekar, N., Magesh, N.S.: Impacts of wave energy and littoral currents on shoreline erosion/ accretion along the south-west coast of Kanyakumari, Tamil Nadu using DSAS and geospatial technology, Environ Earth Sci., doi: 10.1007/s12665-013-2845-6, 2013a.
6. Kaliraj, S., Chandrasekar, N., Magesh, N.S.: Evaluation of coastal erosion and accretion processes along the southwest coast of Kanyakumari, Tamil Nadu using geospatial techniques, Arab J Geosci., doi: 10.1007/s12517-013- 1216-7, 2013b.
7. Kaliraj, S., Chandrasekar, N.: Spectral recognition techniques and MLC of IRS P6 LISS III image for coastal landforms extraction along South West Coast of Tamilnadu, India, BonfringInt J Adv Image Process, 2(3), 01–07, 2012.
8. Katlane, R., Nechad, B., Ruddick, K., Zargouni, F.: Optical remote sensing of turbidity and total suspended matter in the Gulf of Gabes, Arab J Geosci, 6, 1527–1535, 2013.
9. Marcus, W.A., and Fonstad, M.A.: Remote sensing of rivers: the emergence of a subdiscipline in the river sciences, Earth Surface Processes and Landforms, 35(15), 1867–1872, 2010.
10. Nechad, B., Ruddick, K., Park, Y.: Calibration and validation of a generic multi-sensor algorithm for mapping of total suspended matter in turbid waters, Remote Sensing of Environment, 114, 854–866, 2010.
11. Neukermans, G., Ruddick, K., Bernard, E., Ramon, D., Nechad, B., Deschamps, P.Y.: Mapping total suspended matter from geostationary satellites: a feasibility study with SEVIRI in the Southern North Sea, Opt. Express 17, 14029–14052, 2009.
12. Ontowirjo, Budianto, Paris, Rapha, Mano, Akira: Modeling of coastal erosion and sediment deposition during the 2004 Indian Ocean tsunami in Lhok Nga, Sumatra, Indonesia, Natural Hazards, 65(3),1967-1979, 2013.

13. Panwar, S., Agarwal, V., Chakrapani, G. J.: Morphometric and sediment source characterization of the Alaknanda river basin, headwaters of river Ganga, India,Natural Hazards, 1-23, 2017.
14. Qu, L.: Remote sensing suspended sediment concentration in the Yellow River, Ph.D. dissertation paper 383, University of Connecticut, website accessed December 2014 at http://digitalcommons.uconn.edu/dissertations/383/, 2014.
15. Rawat, Pradeep K., Tiwari, P. C., Pant, C. C., Sharama, A. K., Pant, P. D.: Modelling of stream run-off and sediment output for erosion hazard assessment in Lesser Himalaya: need for sustainable land use plan using remote sensing and GIS: a case study, Natural Hazards, 59 (3), 1277-1297, 2011.
16. Sinha, P. C., Guliani, Pragya, Jena, G. K., Rao, A. D., Dube, S. K., Chatterjee, A. K., Murty, Tad : A Breadth Averaged Numerical Model for Suspended Sediment Transport in Hooghly Estuary, East Coast of India, Natural Hazards, 32(2), 239-255, 2004.
17. Tassan, S.: A procedure to determine the particulate content of shallow water from Thematic Mapper data, Int J Rem Sens., 19, 557–562, 1998.
18. Vanhellemont, Q., Neukermans, G., Ruddick, K.: Synergy between polar-orbiting and geostationary sensors: Remote sensing of the ocean at high spatial and high temporal resolution, Remote Sens. Environment, 146, 49–62, 2014.
19. Wang, J.J., and Lu, X.X.: Estimation of suspended sediment concentrations using Terra MODIS: an example from the Lower Yangtze River, China, Science of the Total Environment 408, (5), 1131–1138, 2010.
20. Wang, J.J., Lu, X.X., Liew, S.C., Zhou, Y.: Retrieval of suspended sediment concentrations in large turbid rivers using Landsat ETM plus : an example from the Yangtze River, China, Earth Surface Processes and Landforms, 34, 1082-1092, 2009.
21. Warrick, J.A., Merters, L.A.K., Siegel, D.A., Mackenzie, C.: Estimating suspended sediment concentrations in turbid coastal waters of the Santa Barbara Channel with SeaWiFS, Int J Rem Sens., 25, 1995–2002, 2004.
22. Whitelock, C.H., Witte, W.G., Taly, T.A., Morris, W.D., Usry, J.W., Poole, L.R.: Research for reliable quantification of water sediment concentrations from multispectral scanner remote sensing data. US National Aeronautics and Space Administration, Langley Research Center, Hampton, VA, NASA-TM-82372, 243-255, 1981.
23. Yanjiao, W., Feng, Y., Peiqun, Z., Wenjie, D.: Experimental research on quantitative inversion models of suspended sediment concentration using remote sensing technology, Chinese Geograph Sci.,17 (3), 243–249, 2007.
24. Zhang, Y., Pulliainen, J., Koponen, S., Hallikainen, M.: Water quality retrievals from combined Landsat TM data and ERS-2 SAR data in the Gulf of Finland, IEEE Trans Geosci Remote Sens., 41, 622-629, 2003.

List of Figures

Ocean Sci. Discuss., https://doi.org/10.5194/os-2017-86
Manuscript under review for journal Ocean Sci.
Discussion started: 21 June 2018

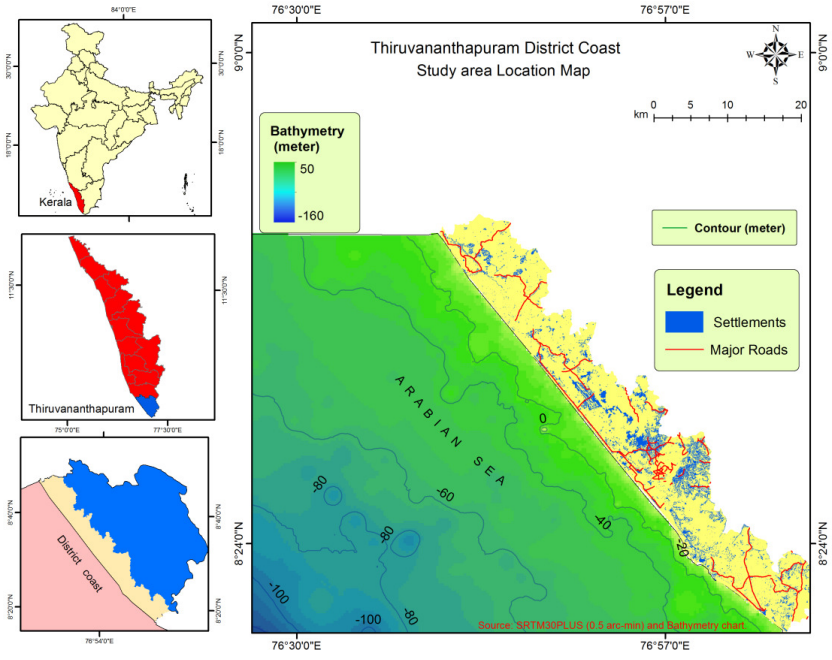

Figure1: Location map of study area.

Ocean Sci. Discuss., https://doi.org/10.5194/os-2017-86
Manuscript under review for journal Ocean Sci.
Discussion started: 21 June 2018

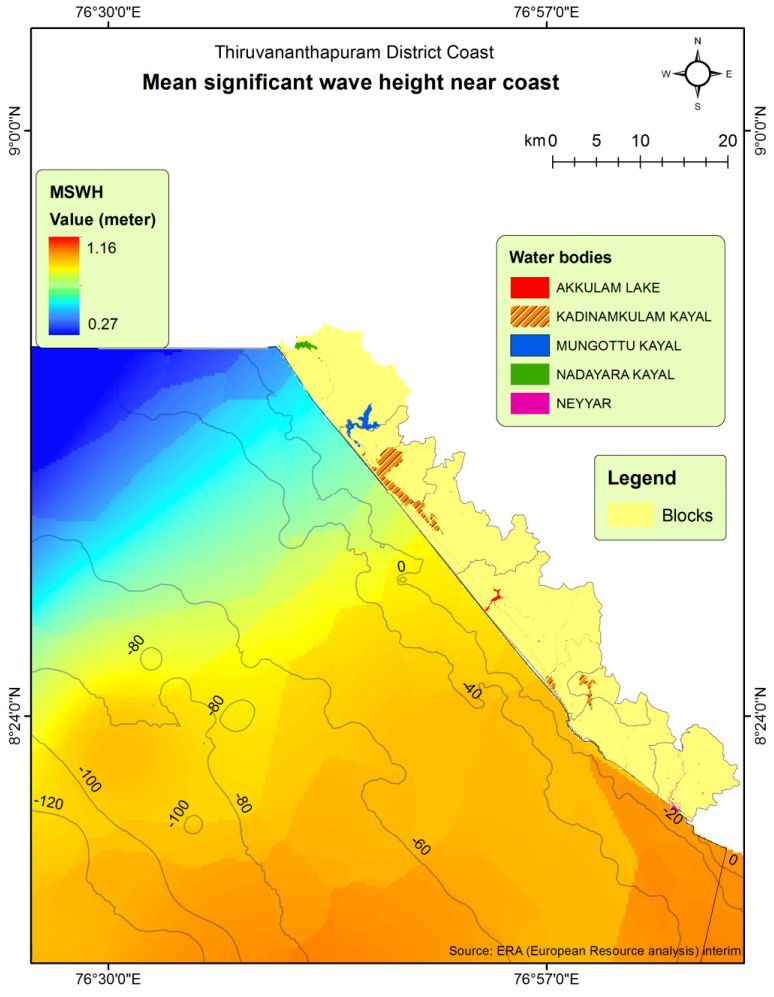

Figure 2: Mean significant wave height along the coast.

Ocean Sci. Discuss., https://doi.org/10.5194/os-2017-86
Manuscript under review for journal Ocean Sci.
Discussion started: 21 June 2018

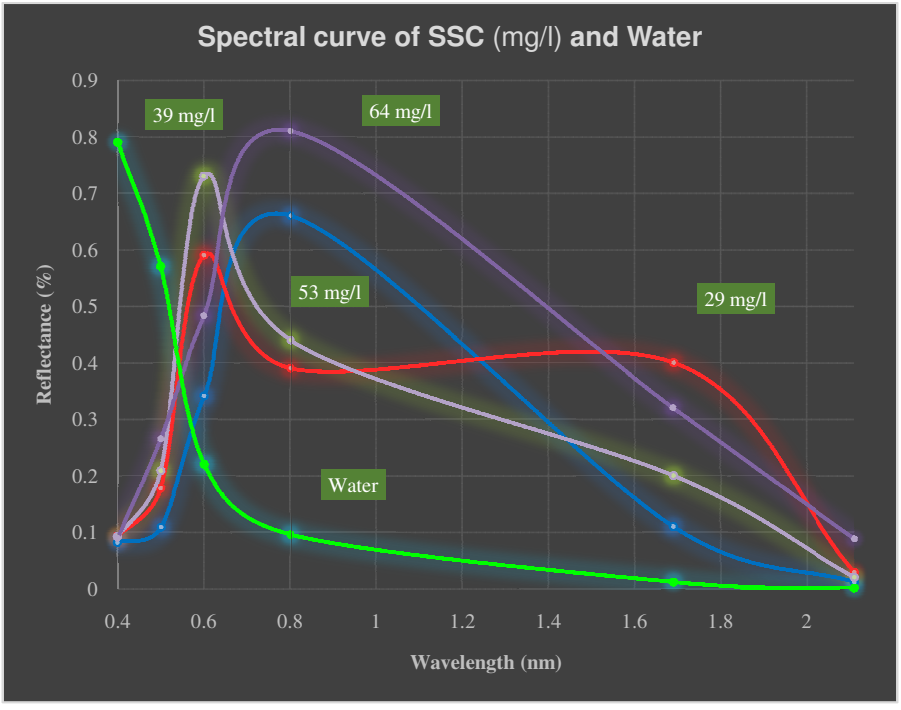

Figure 3: Spectral reflectance curve.

Ocean Sci. Discuss., https://doi.org/10.5194/os-2017-86
Manuscript under review for journal Ocean Sci.
Discussion started: 21 June 2018

Ocean Science
Discussions
Open Access
EGU

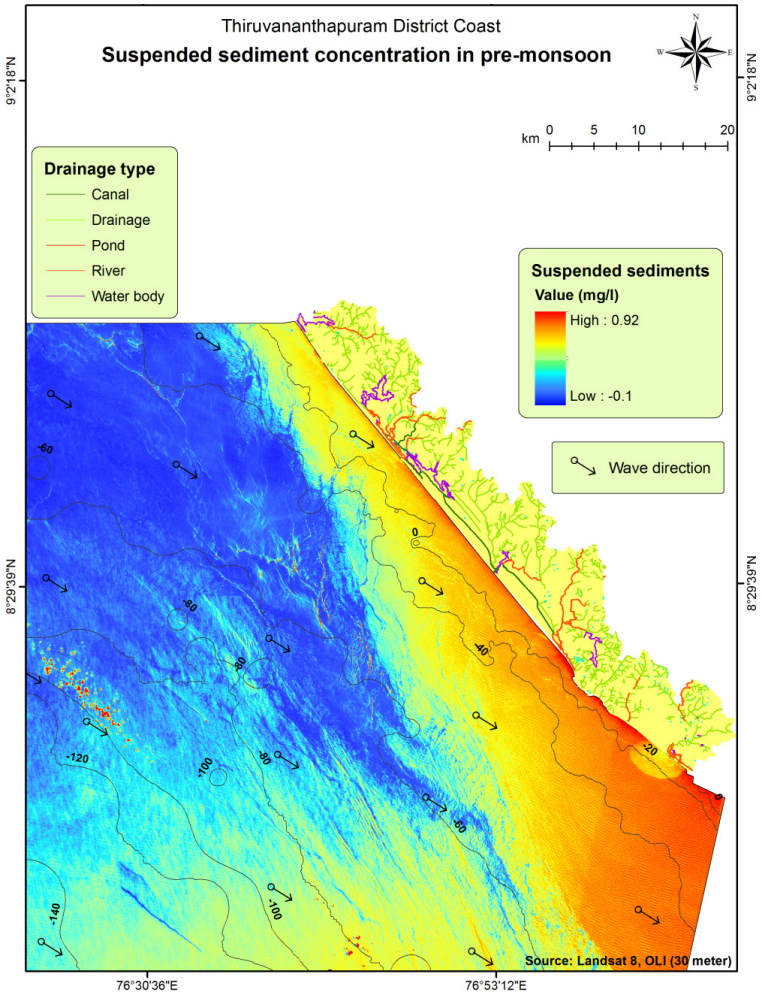

358
359
360 **Figure 4: Suspended sediments in the pre monsoon.**

Ocean Sci. Discuss., https://doi.org/10.5194/os-2017-86
Manuscript under review for journal Ocean Sci.
Discussion started: 21 June 2018

Ocean Science
Discussions
Open Access
EGU

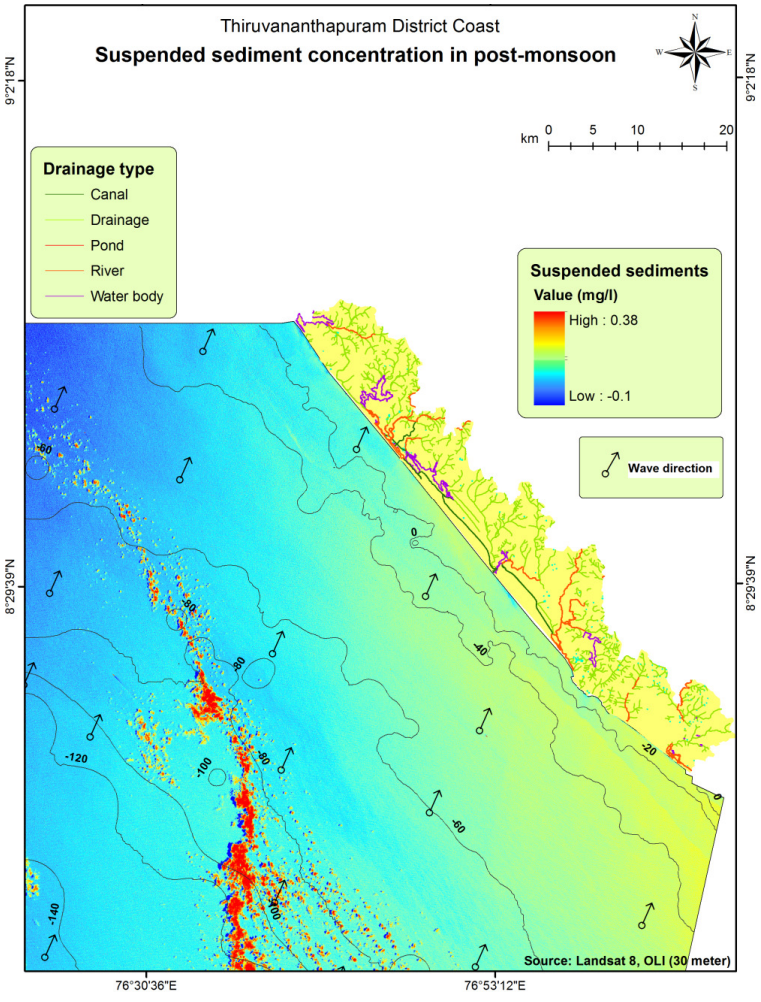

Figure 5: Suspended sediments in the post-monsoon.